

Identifying potential porphyry Cu mineralization at the Kirazlı district in Biga Peninsula (NW Turkey): Insights from the mapping hydrothermal alteration by using shortwave infrared (SWIR) spectrometry

Ali ALUÇ*, Department of Geological Engineering, Muğla Sıtkı Koçman University, Turkey
Department of Earth Sciences, University of Geneva, Switzerland, alialuc@mu.edu.tr; ali.aluc@etu.unige.ch

( <https://orcid.org/0000-0001-6766-8118>)

İlkay KUŞCU, Department of Geological Engineering, Muğla Sıtkı Koçman University, Turkey, ikuscu@mu.edu.tr

( <https://orcid.org/0000-0003-4037-5002>)

Robert MORITZ, Department of Earth Sciences, University of Geneva, Switzerland, robert.moritz@unige.ch

( <https://orcid.org/0000-0003-4299-3250>)

Received: 20.01.2023, Accepted: 14.04.2023

Research Article

*Corresponding author

DOI: 10.22531/muglajsci.1239877

Abstract

The Kirazlı mineral district is located at the center of the Biga peninsula metallogenic province, in a geological setting characterized by an extensional tectonic environment. The district hosts a high-sulfidation (HS) ore body with a total reserve of 33.86 Mt @ 0.69 g/t Au and 9.42 g/t Ag within a large-scale hydrothermal alteration. Although the ideal magmatic-hydrothermal models present the spatial and temporal association of HS-epithermal and porphyry Cu deposits, the porphyry Cu potential at the Kirazlı has not been evaluated, yet. Therefore, the mineral-based alteration mapping with the help of SWIR reflectance spectroscopy was carried out. Our study demonstrates that nine different mineral zone have been distinguished and mapped: (1) Silicification, (2) Alunite, (3) Kaolinite, (4) Dickite, (5) Illite, (6) Pyrophyllite, (7) Chlorite, (8) Sericite, and (9) Montmorillonite zones. Collectively, these alterations exhibit a zoned pattern, from central massive silicification to residual silica, NW-SE oriented alunite, and marginal montmorillonite-illite zones within widespread kaolinite – dickite dominated alteration in Kirazlı main zone. The occurrence of pyrophyllite and sericite dominates at the SE of the Kirazlı district, which refers to relative temperature increase. Subsequent drilling confirms the potential for deep prospecting of porphyry Cu mineralization in the region.

Keywords: Alteration, SWIR, Porphyry Cu, High Sulfidation, Kirazlı, Biga Peninsula

Biga Yarımadası'ndaki Kirazlı bölgesinde potansiyel porfiri bakır mineralizasyonunun belirlenmesi: Kısa dalga kızılötesi (SWIR) spektrometrisi çalışması

Özet

Kirazlı maden bölgesi, Biga yarımadasının metalojenik kuşağının merkezinde, genişlemeli tektonik ortamda oluşmuştur. Bölge, büyük ölçekli bir hidrotermal alterasyon içinde yer alan toplam rezervi 33,86 Mt @ 0,69 g/t Au ve 9,42 g/t Ag olan yüksek sülfidasyonlu (HS) epitermal bir cevher kütlesine ev sahipliği yapmaktadır. İdeal magmatik-hidrotermal modeller, HS-epitermal ve porfiri bakır yataklarının mekansal ve zamansal ilişkisini sunsa da, Kirazlı'daki porfiri bakır cevherleşmesi potansiyeli henüz değerlendirilmemiştir. Bu nedenle, SWIR spektroskopisi yardımıyla mineral bazlı alterasyon haritalaması gerçekleştirilmiştir. Çalışmamız dokuz farklı mineral zonunun ayırt edildiğini ve haritalandığını göstermektedir: (1) Silisleşme, (2) Alunit, (3) Kaolinit, (4) Dikit, (5) İllit, (6) Pirofilit, (7) Klorit, (8) Serisit ve (9) Montmorillonite zonları. Toplu olarak, bu alterasyonlar, Kirazlı ana zonundaki yaygın kaolinit-dikit baskın alterasyon içinde, merkezi masif silisleşmeden, KB-GD yönlü alünit ve marjinal montmorillonit-illit zonlarına kadar bir zonlanma modeli sergilemektedir. Kirazlı bölgesinin güneydoğu'sunda ise pirofilit ve serisit minerallerinin hakim olması sıcaklık artışını ifade ederek potansiyel bir porfiri bakır cevherleşmesini işaret eder. Takibinde yapılan sondaj çalışmaları, bölgedeki porfiri bakır mineralizasyonunun potansiyelini doğrulamaktadır.

Anahtar Kelimeler: Alterasyon, SWIR, Porfiri Cu, Yüksek Sülfidasyon, Kirazlı, Biga Yarımadası

Cite

Aluç, A., Kuşcu, İ., Moritz, R., (2023). "Identifying potential porphyry copper mineralization at the Kirazlı district in Biga Peninsula (NW Turkey): Insights from shortwave infrared (SWIR) spectrometry", *Mugla Journal of Science and Technology*, 9(1), 53-62.

1. Introduction

Short wavelength (range of 1,300 to 2,500 nanometers) infrared (SWIR) reflectance spectroscopy is a highly efficient and low-cost tool for mineral identification in the both field and laboratory with high sampling density. This spectral range includes vibrations of essential absorption characteristics linked to the molecular bonds of OH, H₂O, CO₃, NH₄, AlOH, FeOH, and MgOH [1]. Therefore, it is widely in use for the determination of different mineral groups, including phyllosilicates, hydroxylated silicates and sulfates, carbonates, and ammonium-bearing minerals [2] to create mineral-based alteration maps and models [3-8]. Earlier efforts on ore deposits have concentrated on the alteration of minerals as exploration vectors of mineralization since large-scale hydrothermal alteration is typically associated with mineralization [4, 9, 10]. The ideal magmatic-hydrothermal models present the spatial and temporal association of epithermal and porphyry Cu deposits (PCD). In these models, the high sulfidation (HS) epithermal systems and the PCDs are co-genetic and HS epithermal systems are formed within the advanced argillic alteration zone of porphyry Cu deposits [11]. The coexistence of the epithermal systems with PCD is called the telescoping process, and it describes the juxtaposing or overprinting of early-deep PCD by late-shallow epithermal style mineralization. In the telescoped systems, the HS epithermal systems are presumed to share a common hydrothermal origin with the PCD and are formed by syn-hydrothermal degradation of volcanic paleosurface [11]. Kuşcu [12] documented that some PCDs within western Anatolia are juxtaposed to or spatially associated with the HS epithermal systems of similar age groups (Fig. 1). Yet, no clear constraints on their coexistence have been made by Kuşcu [12]. However, Yiğit [14] reported that some of the high sulfidation epithermal systems are transitional both in the vertical and horizontal extent to porphyry systems in the Biga Peninsula (Fig. 1).

The detailed work on the geology and temporal association of overprinting mineralization styles in individual deposits in the last decade [12, 14-18] revealed that the coexistence of the PCD to HS epithermal systems in the Biga peninsula could be misleading, and telescoped PCDs in the Biga peninsula may be a matter of debate at the present. The main reasons are poorly understood overprinting multiphase ore-forming processes and lack of detailed information on volcanic stratigraphy and correlation due to regional hydrothermal alteration blurring the original nature of host rock units.

Kirazlı is a standalone mining district consisting of five target zones at the center of the Biga Peninsula (Fig. 1) The most promising target zones are Kirazlı main, which hosts a high sulfidation epithermal Au-Ag ore body with a reserve of 33.86 Mt @ 0.69 g/t Au, 9.42 g/t Ag, and a resource of 3.056 Mt @ 0.43 g/t Au, 2.71 g/t Ag [18, 19],

Çatalkaya and Kale (Fig. 2). The exploration program by Alamos Gold in 2013 enabled the intersection of the porphyry Cu style veins and veinlets in a deeper drill, neither the detailed characterization nor the temporal and spatial association of the porphyry Cu with high sulfidation Au-Ag mineralization would become of interest to any further exploration program or research.

In the current study, alteration mapping with the help of short wavelength infrared (SWIR) reflectance spectroscopy was conducted in the Kirazlı district, to identify the types and spatial distribution of hydrothermal alteration. The findings will help to understand the alteration-mineralization processes and provide useful tools for further exploration of a potential porphyry Cu mineralization in the mining district and adjacent regions with a comparable geological-hydrothermal setting.

2. Regional Geology

Biga Peninsula forms the north-western tip of the Anatolian plate, tectonically divided into two flanks. It is situated on a section of the Sakarya zone in the east and the Rhodope-Strandja Massif in the west (Fig. 1). Crystalline basement rocks are composed of NE-trending pre-Permian Kazdağ and Permo-Triassic Çamlıca metamorphic rocks in the Sakarya and Rhodope zones, respectively. These rocks are tectonically overlain by the Permo-Triassic Karakaya complex, which consists of partially metamorphosed volcanic and clastic rocks in the east, and the Cretaceous Çetmi ophiolitic mélange in the north-northwest (Fig. 1) [23, 24]. The Cenozoic geological development of the Biga Peninsula was controlled by four major tectonic events: (1) closure of the Neo-Tethys Ocean during northward subduction, (2) collision of the Anatolide-Tauride Block and the Sakarya zone along the Izmir-Ankara-Erzincan Suture during the late Cretaceous and early Eocene, (3) Post-collisional tectonics from the Eocene to the Middle Miocene, and (4) subduction of the African plate beneath the Eurasian plate, and tectonic escape, which led to a progressive extension in the middle Eocene to recent [13, 25-33]. The extensional deformation helped exhume the basement rocks alongside shallow-dipping detachment faults and to the emplacement of large plutons at shallow depths [12, 23, 34]. Although the timing is not certain and could be either Oligocene [23, 24] or early-middle Miocene, the Biga Peninsula is covered with Cenozoic plutonic and volcanic rocks. The ages of these rocks vary from 52 to 18 Ma, with younger ages toward the southwest [12, 14], with the exception of the pre-Cenozoic plutons near the southern Marmara Sea.

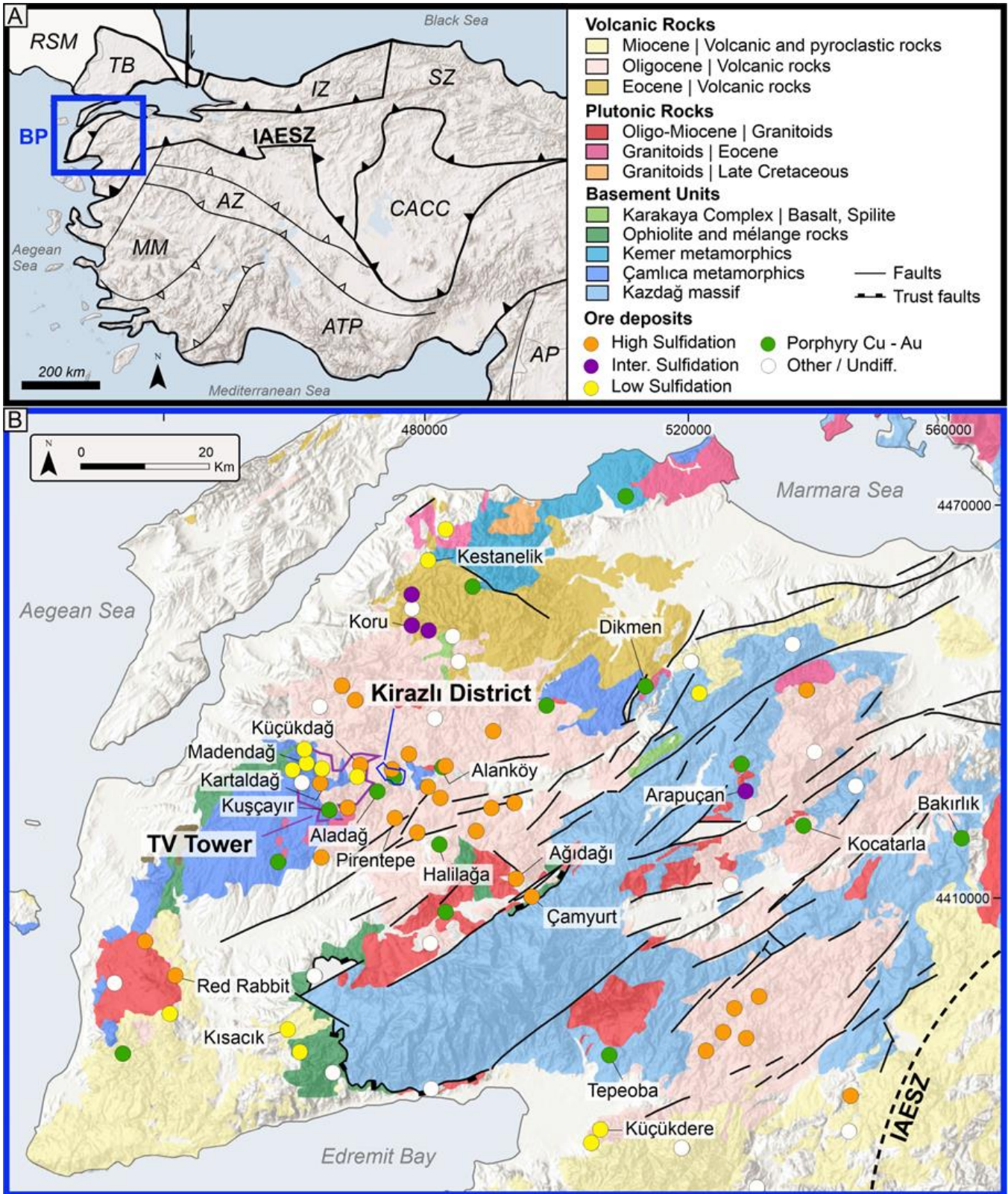


Figure 1. Figure 1. (A) Simplified map showing the tectonic units of western Turkey (modified from [13]; Heavy lines with filled triangles show sutures, and soft lines with open triangles indicate thrust belts; AZ: Afyon Zone, ATB: Anatolide-Tauride Block, AP: Arabian Platform, MM: Menderes Massif, CACC: Central Anatolian Crystalline Complex, IAESZ: Izmir-Ankara-Erzincan Sture Zone, IZ: Istanbul Zone, TB: Thrace Basin, RSM: Rhodope-Strandja Massif, BP: Biga Peninsula, (B) Geological map showing volcanic, plutonic, basement rocks, main structural units and the major ore deposits and occurrences of the Biga Peninsula (simplified from 1/25 K Geological map of Turkey (MTA) and the coordinates for Fig. 1A in decimal degrees and for Fig. 1B in WGS 1984 Zone 35N)

3. Geological Setting of the Kirazlı District

The Permian Çamlıca metamorphics form the basement of the Kirazlı district and are composed of marble blocks and dark grey to grey quartz-mica schist (Fig. 1, 2; [14, 19, 20]). They are mostly observed near the eastern margin of the Kirazlı district, where they are covered by conglomerate and low-grade metamorphosed sandstone-mudstone of the Permo-Triassic Karakaya complex (Fig. 3A). All basement rocks are intruded by the middle Eocene undifferentiated intrusive rocks, which are exposed as isolated bodies to the south of the Kirazlı district. They are called “undifferentiated intrusive rocks” since their severe deformation and alteration, which prevent their compositional and textural properties and make it difficult to identify initial properties (Fig. 3D). The Eocene plagioclase-phyr

andesite (PAnd) and Oligocene basaltic andesite (BAnd) constitute the main volcanic rocks in the Kirazlı district and exposed in the western and central parts, respectively (Fig. 2, 3F-G). The PAnd is non-pervasively altered, light to dark green in color, and partially silicified. The BAnd is mainly gray to green and white in color due to pervasive clay alteration (Fig. 3F-G). They are partially oxidized, silicified, and chloridized, and are equigranular in texture. It is locally intercalated with lithic and subordinate crystal tuff, which are dominantly yellowish-white in color but also occur as red to dark brown colored rocks (with the abundant symmetric layering of different tones of red and brown-like lieegang bands, Fig. 3B-C). The BAnd and pyroclastic rocks are locally brecciated and crop out as small ledges at the topmost levels of the Kirazlı district (Fig. 3B-C).

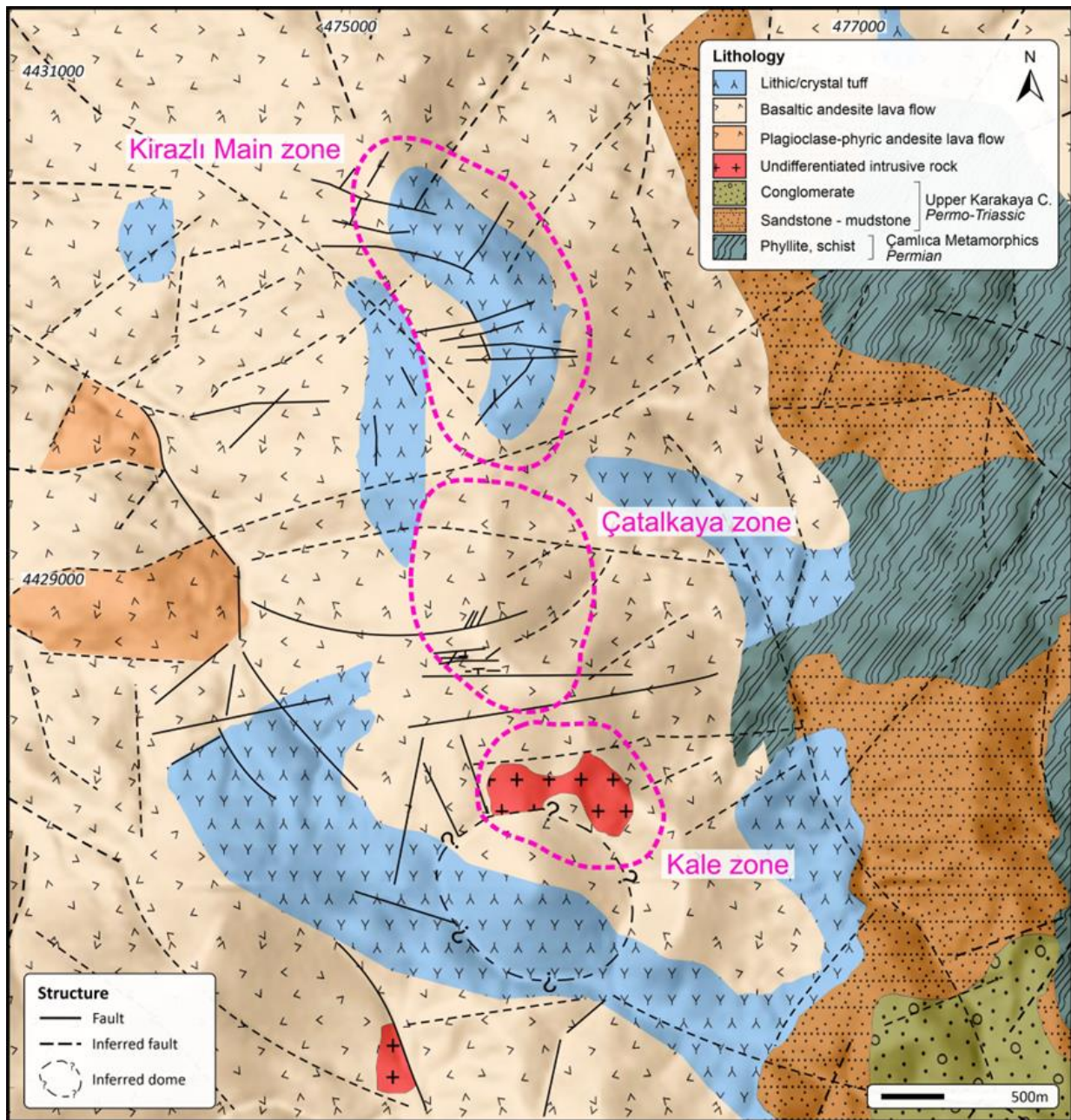


Figure 2. Geological map of the Kirazlı district showing lithological and structural elements

4. Mineralization at the Kirazlı District

The Kirazlı district contains an HS epithermal Au-Ag deposit and porphyry Cu mineralization. The HS epithermal system is hosted by Oligocene partially brecciated, silicified, and oxidized basaltic andesite (BAnd) and crystal tuff. The NNW-SSE trending epithermal ore body lies beneath Kirazlı main zone (Fig. 2). Cunningham-Dunlop and Lee [35] proposed at least four silicification phases in the HS ore body and two main types of gold mineralization concerning the average gold grade [16]. Regional-scale low-grade gold

mineralization associated with low-temperature silica is interpreted to be early and enveloping the high-grade gold mineralization observed at the margins of breccia bodies within an argillic zone. The gold is subsequently enriched by supergene oxidation processes. The porphyry Cu type millimeter-scale dark quartz stockworks overprinted by argillic alteration in the surface of the Kale zone (Fig. 3D-E) reveal the mineralization potential on pervasively altered Eocene undifferentiated intrusive rock and plagioclase-phyric andesitic lava flow (PAnd).

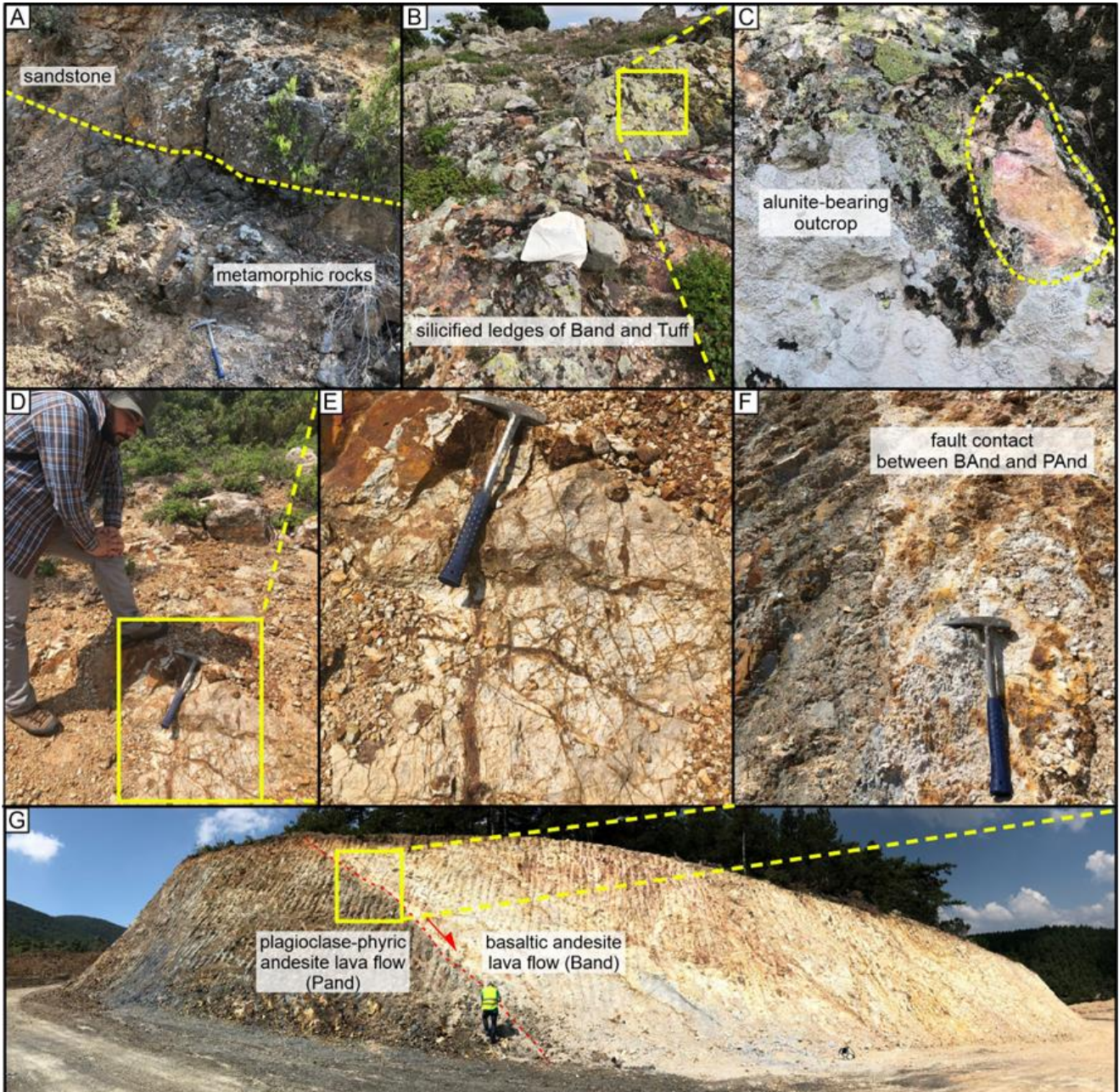


Figure 3. Field relationships of the Kirazlı district. (A) contact relationship between basement metamorphic rocks and sandstone-mudstone of the Karakaya complex, (B-C) partially brecciated and silicified ledges of the BAnd and lithic tuff at the top of Kirazlı main zone, inset photo, representing alunite-bearing zone in silicified ledges, (D-E) undifferentiated intrusive unit hosting quartz stockworks at the Kale zone, inset photo, close view of the quartz stockworks, (F-G) Field exposure of the BAnd and PAnd contact at the shallower elevations of the Çatalkaya Zone, inset photo, close view of the contact.

5. Methodology

5.1. SWIR Spectral Analysis

5.1.1. Background

The SWIR spectrum (1100-2500 nm) is an electromagnetic wave that occurs between the near-infrared (800-1100 nm) and mid-infrared (MWIR, 3000-5000nm) spectrums as a result of molecular stretching and bending vibration or electron orbital transition of the electron layer [3]. Various functional groups or chemical bonds can only absorb light energy at a certain wavelength, resulting in distinctive infrared absorption peaks. The mineral may preferentially absorb the spectrum energy at this frequency when a light beam with the same frequency as the functional group causes a resonance occurrence. Therefore, the infrared spectrum curve can record the composition and structure of the mineral(s), which form the rock [37]. The spectrum matching and fitting in the established standard mineral spectral library can reveal the mineral composition and relative content in the rock can be determined qualitatively according to the position of the characteristic absorption peak, and the depth of the absorption peak, respectively [37]. Many functional groups, including OH (Al-OH, Fe-OH, Mg-OH), H₂O, NH₄, CO₃, and SO₄ can produce characteristic absorption wavelengths (Fig. 4).

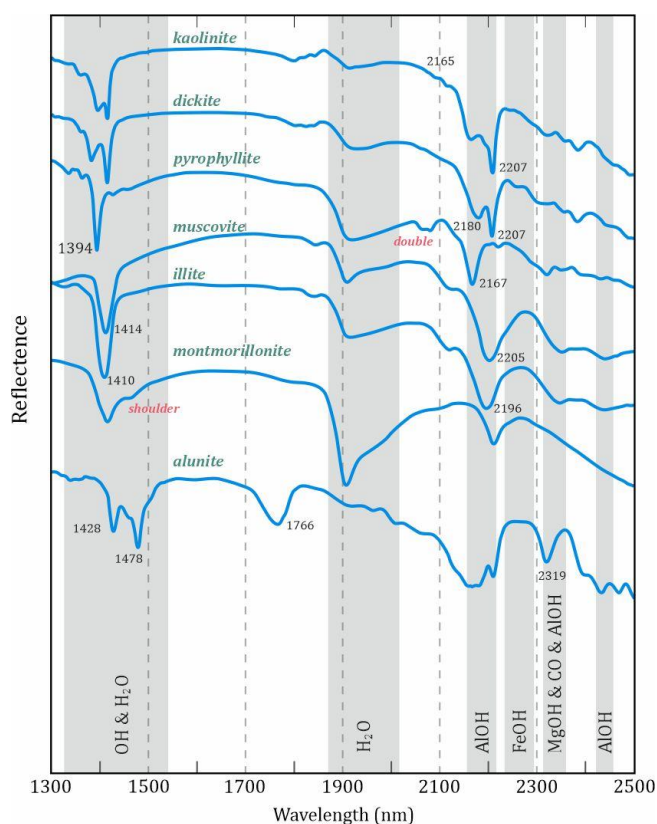


Figure 4. Characteristic SWIR absorption features in spectra of kaolinite, dickite, pyrophyllite, muscovite, illite, montmorillonite and alunite (modified after [37]).

Therefore, SWIR spectral analysis can identify mineral groups such as hydroxyl silicate minerals (white mica, biotite, chlorite, pyrophyllite, etc), sulfate minerals (alunite, anhydrite, etc.), and carbonate minerals [3] since they have characteristic spectrums (Fig. 4). For instance, the white mica has three main absorption features at ~2200 nm (usually used as the diagnostic absorption feature due to the sharp, deep, single Al-OH absorption feature), ~1900 nm (H₂O), and ~1400 nm (H₂O + OH) (Fig. 4, [3 and reference therein]). The primary absorption features can be affected by other minerals, which have the same absorption feature at the same wavelength. For instance, the chlorite has absorption features at ~1400 nm (OH), ~2000 nm, 2195 nm (Al-OH), and diagnostic ~2250 nm (Fe-OH,) and ~2340 nm (Mg-OH) (Fig. Y, [38,39]). The absorption feature of the Mg-OH at ~2340 nm can easily be affected by epidote, calcite, and white mica, which all exhibit the same absorption feature. Thus, the secondary absorption feature at ~2250 nm is usually used in the determination. [39 and reference therein].

5.1.2. Field Studies and Sampling

The field study was performed in and around the Kirazlı district in two different sessions. Fourteen different traverses (35 km in total) were created to cover the entire Kirazlı district. The systematic sampling was conducted every 50m unless the alteration shifted rapidly or the lithology changed. In total 530 samples were collected. Additionally, Alamos Gold INC. shared earlier SWIR studies, which had been conducted on 695 soil samples.

5.1.3. Data Processing

Spectral analyses were conducted indoors with the help of ASD TerraSpec 4 Hi-Res mineral analyzer. The effective wavelength range was 350–2500 nm, and the ASD-calibrated white panel was used as the reflectivity reference standard. The integral time of the spectral measuring point was 100 milliseconds with a resolution of 3nm at 700nm and 6nm at 1400/2100nm. The device measures with three detectors as VNIR (350-1000nm), SWIR 1 (1001-1800nm), and SWIR 2 (1801-2500nm), with a wavelength accuracy of 0.5nm [21]. After cleaning and drying (45° in 24 hours), the samples were analyzed three times with their surfaces (X, Y, Z) to crosscheck mineral content.

Based on the physical mechanism of the mineral spectral reaction, the Spectral Geologist software (TSG 8.0 version) created by the Commonwealth Scientific and Industrial Research Organization of Australia (CSIRO) was utilized to determine mineral information directly from spectral curves [22] after noise reduction and background removal. The extracting results were further examined and filtered manually to reduce the interference between different minerals with overlapping absorption bands (Fig. 5). The complete list of SWIR data together with sample locations is given in Appendix A.

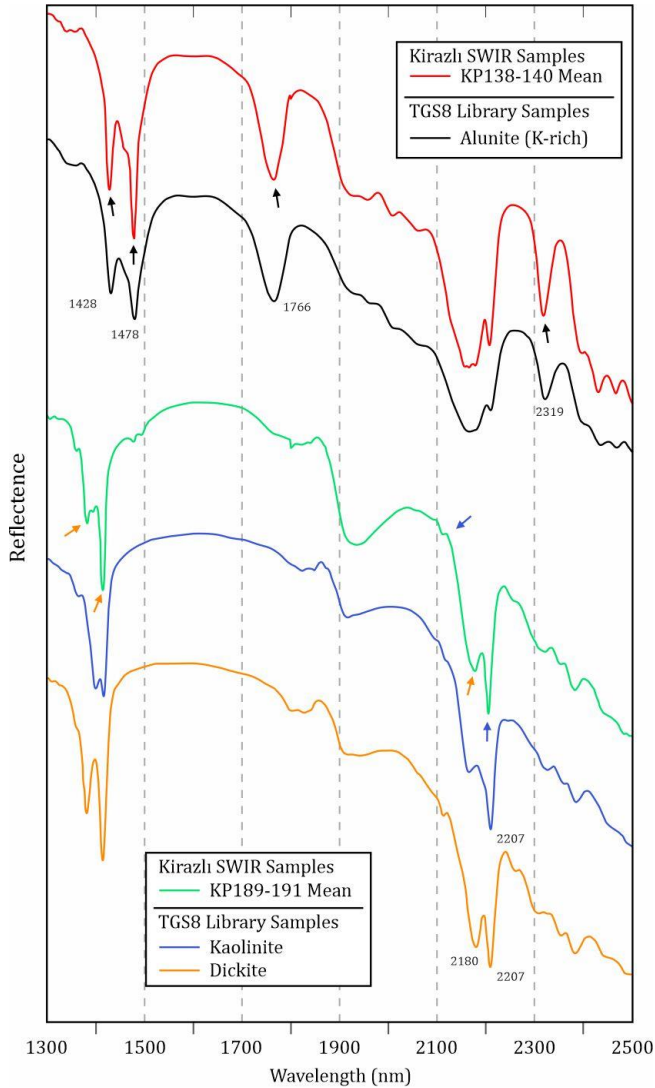


Figure 5. The comparison and fitting of the SWIR absorption features of selected samples from Kirazlı district (KP138-140M, KP189-191M) with TGS8 library samples (alunite, kaolinite, dickite).

6. Results and Discussion

6.1. Hydrothermal Alteration as a Proxy of Blind Mineralization at the Kirazlı District

The hydrothermal alteration in the Kirazlı district is strongly pervasive and widespread. The relationships between alteration assemblages are too complex to identify individually due to the superimposition of different alterations. Therefore, the shortwave infrared reflectance (SWIR) spectral analyzer was used to create a mineral-based alteration map of the district (Fig. 6-7). Based on the spatial distribution and predominance of minerals, nine different mineral zone have been distinguished and mapped: (1) Silicification, (2) Alunite, (3) Kaolinite, (4) Dickite, (5) Illite, (6) Pyrophyllite, (7) Chlorite, (8) Sericite, and (9) Montmorillonite zones. Collectively, these alterations exhibit a zoned pattern, from central massive silicification to residual silica (vuggy quartz), NW-SE oriented alunite, and marginal montmorillonite-illite zones within widespread kaolinite

– dickite dominated alteration in Kirazlı main zone. Whereas, pyrophyllite and sericite (mainly muscovite and illite) dominated alteration are pronounced in Çatalkaya and Kale zones (Fig. 7).

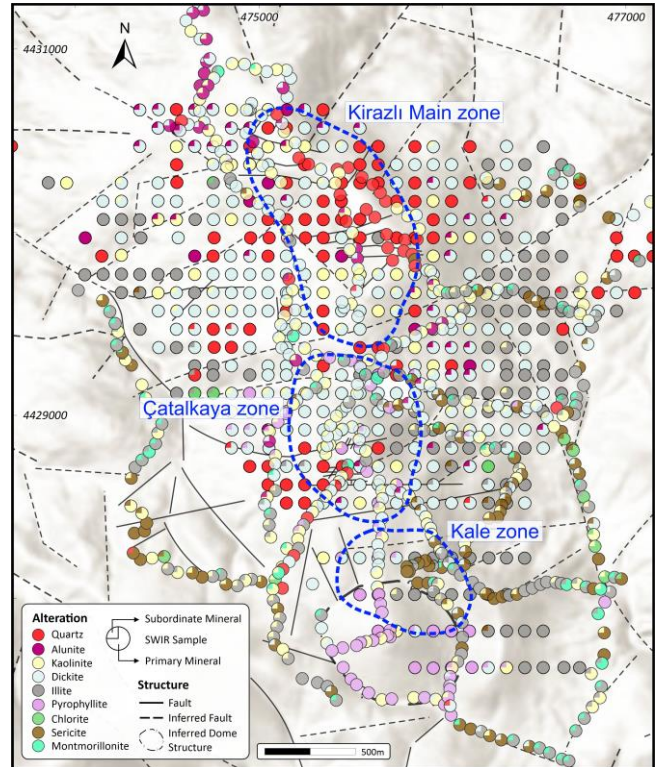


Figure 6. Sample locations with SWIR readings consist of primary and subordinate hydrothermal alteration minerals.

Silicification is the most common alteration type in the Kirazlı district and outcrops as brecciated and massive bodies along the ridges of Kirazlı main and Çatalkaya zones. This alteration is represented by pale to dark grey, occasionally reddish in color, massive to residual silica (vuggy quartz), and subordinate sugary in texture. The silicification can be followed up to the first 100 m below the surface on top of argillic alteration at Kirazlı main zone and locally related to ENE-WSW trending structural controls in the Çatalkaya zone. The alunite-dominated alteration occurs within the NW-SE corridor at Kirazlı main zone and patchily surrounds the silicification as fine-grained disseminations and small pinkish veins in the northern part of the Kirazlı main zone. Kaolinite is the most widespread alteration mineral that covers extensive areas in the Kirazlı district. Whereas dickite is more abundant in Kirazlı main and Çatalkaya zones. Illite and montmorillonite as well as chlorite form marginal alterations in the Kirazlı district.

The occurrence of pyrophyllite refers to a relative temperature increase and represents a transition from an epithermal to a porphyry environment. The pyrophyllite and sericite (mainly muscovite with less abundant illite) are dominant from the Çatalkaya zone to the south of the Kirazlı district, respectively, and the prominent, sericitic alteration observed in drill holes located at the Kale zone (Fig. 7). In parallel, sericite

intersected deeper levels of the drill holes in the south of Kirazlı main zone. Lacking deep drill holes in the Çatalkaya zone beclouds the alteration correlation between Kirazlı main and Kale zones, more clearly epithermal and porphyry environment. The sericitic alteration exposed in shallow levels is pervasively overprinted by widespread kaolinite and dickite dominated argillic alteration.

On the other hand, 8 follow-up drilling conducted at the Kale zone to test sericite pyrophyllite-dominated alteration zone at the surface. Sericitic alteration is

dominantly observed in drill holes and pervasively overprint potassic alteration in shallow levels (Fig. 8A). Despite the well-developed quartz-sulfide veins (Fig. 8B) during potassic alteration, very limited intersections exhibit minerals forming potassic alteration such as secondary-biotite and potassium feldspar. The distribution and zonation of predominant alteration minerals from Kirazlı main zone towards the Kale zone represent a typical transition of high sulfidation epithermal to porphyry environments.

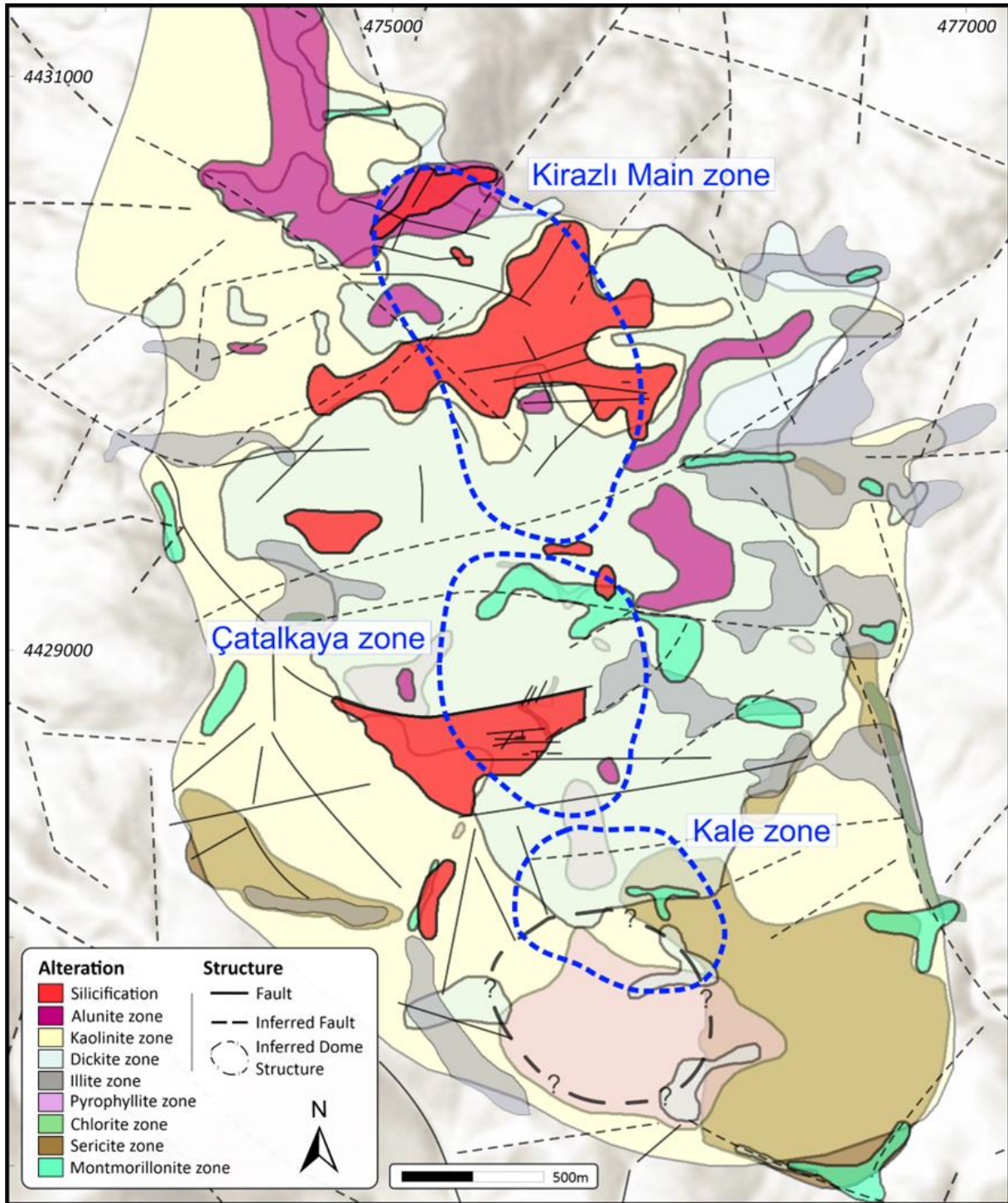


Figure 7. Mineral-based alteration map of the Kirazlı district.

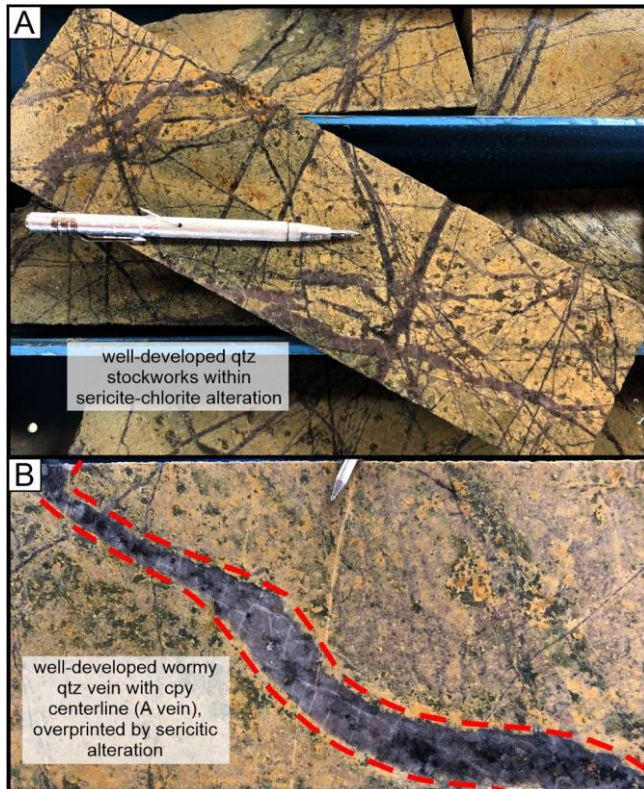


Figure 8. Drill core samples from the Kale zone, (A) well-developed quartz stockworks within sericite-chlorite alteration, (B) well-developed wormy quartz vein with chalcopyrite centerline (A vein) overprinted by sericitic alteration.

7. Conclusion

The Kirazlı district developed a magmatic-hydrothermal mineralization system with the potential for blind porphyry Cu deposits in the south. Mineral mapping using SWIR reflectance spectroscopy was conducted and the zonation of the hydrothermal alteration shows a shift from low to moderate temperature from north to south. The domination of pyrophyllite and sericite in Çatakaya and Kale, respectively, suggest a typical transition of high sulfidation epithermal to porphyry environments. In conclusion, the presence of porphyry-type alteration and HS-type mineralization suggests the potential for further prospecting in the Kirazlı district.

8. Acknowledgments

This study is a chapter of A. Aluç's Ph.D. thesis as part of the joint Ph.D. program between Mugla and Geneva Universities. It was supported by Doğu Biga Madencilik subsidiary of Alamos Gold INC. and the Scientific and Technological Research Council of Turkey (TÜBİTAK) under the framework of the 2214A scholarship program. Senior Geologist Gülsevım Özışık, Field assistants Nazım Tomruk, and Sefer Sezgin are acknowledged for their help during fieldwork. We are grateful to Exploration Director Mehtap Karıcı for the legal permissions and technical help.

9. References

- [1] Thompson, A.J.B., Hauff, P.L. and Robitaille, A.J., "Alteration mapping in exploration: application of shortwave infrared (SWIR) spectroscopy", *Society of Economic Geologists Newsletter*, 39, 16–27, 1999.
- [2] Pontual, S., Merry, N. and Gamson, P., "Spectral interpretation field manual", *G-MEX: Arrowtown, New Zealand, AusSpec International Pty. Ltd.*, Unpublished manual, 168 p., 1997.
- [3] Mathieu, M., Roy, R., Launeau, P., Cathelineau, M., Quirt, D., "Alteration mapping on drill cores using a HySpex SWIR-320m hyperspectral camera: application to the exploration of an unconformity-related uranium deposit (Saskatchewan, Canada)", *Journal of Geochemical Exploration*, 172, 71–88, 2017.
- [4] Testa, F.J., Villanueva, C., Cooke, D.R., Zhang, L.J., "Lithological and hydrothermal alteration mapping of epithermal, porphyry and tourmaline breccia districts in the argentine Andes using ASTER imagery", *Remote Sensing*, 10, 203, 2018.
- [5] Huang, J., Chen, H., Han, J., Deng, X., Lu, W., Zhu, R., "Alteration zonation and short wavelength infrared (SWIR) characteristics of the Honghai VMS Cu-Zn deposit, Eastern Tianshan, NW China", *Ore Geology Reviews*, 100, 263–279, 2018.
- [6] Zhou, Y., Li, L.M., Yang, K., Xing, G.F., Xiao, W.J., Zhang, H.L., Xiu, L.C., Yao, Z.Y., Xie, Z.J., "Hydrothermal alteration characteristics of the Chating Cu-au deposit in Xuancheng City, Anhui Province, China: significance of sericite alteration for Cu- au exploration", *Ore Geology Reviews*, 127, 103844, 2020.
- [7] Zhou, Y., Chen, S., Li, L., Fan, F., Zhang, H., Chen, J., Yang, K., Xiu, L., Xu, M., & Xing, G., "Mapping hydrothermal alteration of the Au-Cu deposits in the Zhenghe magmatic-hydrothermal mineralization system, SE China, using Short Wavelength Infrared (SWIR) reflectance spectroscopy" *Journal of Geochemical Exploration*, 244, 107113, 2023.
- [8] Sönmez, Ş.U., Kuşçu, İ. "Geology, geochemistry, geochronology and genesis of the late Miocene porphyry Cu-Au-Mo mineralization at Afyon-Sandıklı (AS) prospect, western Anatolia, Turkey", *Ore Geology Reviews*, 121, 2020.
- [9] Zadeh, M.H., Tangestani, M.H., Roldan, F.V., Yusta, I., "Spectral characteristics of minerals in alteration zones associated with porphyry copper deposits in the middle part of Kerman copper belt, SE Iran", *Ore Geology Reviews*, 62, 191–198, 2014.
- [10] Li, Y., Su, C., Wang, X., Huang, Z., Zhang, X., "Extraction of alteration information and establishment of prospecting model for porphyry copper-gold deposits in Luzon", *Remote Sensing Technology and Application*, 6, 1151–1160, 2017.
- [11] Sillitoe, R.H., "Porphyry Copper Systems*", *Economic Geology*, 105, 3–41, 2010.
- [12] Kuşçu, İ., Tosdal, R. M., and Gençalioglu-Kuşçu, G., "Episodic porphyry Cu (-Mo-Au) formation and

- associated magmatic evolution in Turkish Tethyan collage". *Ore Geology Reviews*, 107, 119-154, 2019.
- [13] Okay, A. I., and Tüysüz, O., "Tethyan sutures of northern Turkey", *Geological Society, London, Special Publications*, 156(1), 475, 1999.
- [14] Yigit, O., "A prospective sector in the Tethyan Metallogenic Belt: Geology and geochronology of mineral deposits in the Biga Peninsula, NW Turkey", *Ore Geology Reviews*, 46, 118-148, 2012.
- [15] Brunetti, P., Magmatic-hydrothermal evolution and post-ore modifications of the Halilağa porphyry Cu-Au deposit, NW Turkey, University of British Columbia, Vancouver, Canada 2016.
- [16] Leroux, G., M., Stratigraphic and petrographic characterization of HS epithermal Au-Ag mineralization at the TV Tower district, Biga Peninsula, NW Turkey, University of British Columbia, Vancouver, Canada, 2016.
- [17] Sánchez, M. G., McClay, K. R., King, A. R., and Wijbrams, J. R. (Editor, J. P. Richards), "Cenozoic Crustal Extension and Its Relationship to Porphyry Cu-Au-(Mo) and Epithermal Au-(Ag) Mineralization in the Biga Peninsula, Northwestern Turkey", *Tectonics and Metallogeny of the Tethyan Orogenic Belt (Vol. 19)*, 2016.
- [18] Aluç, A., Kuşcu, I., Ulianov, A., Selby, D., Antoine, C., Spikings, R., and Moritz, R., "Protracted metallogenic and magmatic evolution of the epithermal Au-Ag and porphyry Cu deposits at the Kirazlı district, Biga Peninsula, NW Turkey: Evidence from zircon U-Pb, muscovite $^{40}\text{Ar}/^{39}\text{Ar}$, and molybdenite Re-Os geochronology", *Mineralium Deposita*, in press.
- [19] Cormier, A., Jutras, M., Welhener, H., Minard, T., Chiaramello, P., Cremeens, J., NI 43-101 Technical Report Feasibility Study Technical Report on the Kirazlı Project, Çanakkale Province, Turkey, 2017.
- [20] Smith, M., T., Lepore, W., A., Incekaraoğlu, T., Shabestari, P., Boran, H., Raabe, K., "Küçükdağ: A New, High Sulfidation Epithermal Au-Ag-Cu Deposit at the TV Tower Property in Western Turkey", *Economic Geology*, 109(6), 1501-1511, 2014.
- [21] ASD TerraSpec 4 Hi-Res mineral analyzer Specifications, 2023, Retrieved from: https://www.malvernpanalytical.com/en/assets/P/N13063_BR_ASD%20Terraspec%204%20Hi%20Res%20brochure_EN_tcm50-61713.pdf.
- [22] Yang, K., Whitbourn, L., Mason, P., Huntington, J., "Mapping the chemical composition of nickel laterites with reflectance spectroscopy at Koniambo, New Caledonia", *Economic Geology*, 6, 1285-1299, 2013.
- [23] Okay, A.I., Satir, M., "Coeval plutonism and metamorphism in a latest Oligocene metamorphic core complex in northwest Turkey" *Geological Magazine*, 137(5), 495-516, 2000.
- [24] Bonev, N., Beccaletto, L., "From syn- to post-orogenic Tertiary extension in the north Aegean region: constraints on the kinematics in the eastern Rhodope-Thrace, Bulgaria-Greece and the Biga Peninsula, NW Turkey", *Geological Society, London, Special Publications*, 291(1), 113-142, 2007.
- [25] McKenzie, D., "Active tectonics of the Alpine-Himalayan belt: the Aegean Sea and surrounding regions", *Geophysical Journal International*, 55(1), 217-254, 1978.
- [26] Le Pichon, X., Angelier, J., "The Hellenic arc and Trench System: A key to the Neotectonic Evolution of the Eastern Mediterranean", *Tectonophysics*, 60, 1-42, 1979.
- [27] Şengör, A.M.C., Yılmaz, Y., "Tethyan Evolution of Turkey" *Tectonophysics*, 75, 181-241, 1981.
- [28] Meulenkamp, J.E., Wortel, M.J.R., Van Wamel, W.A., Spakman, W., Strating, E.H., "On the Hellenic subduction zone and the geodynamic evolution of Crete since the late Middle Miocene", *Tectonophysics*, 146(1-4), 203-215, 1988.
- [29] Harris, N.B.W., Kelley, S., Okay, A.I., "Post-collision magmatism and tectonics in northwest Anatolia", *Contributions to Mineralogy and Petrology*, 117(3), 241-252, 1994.
- [30] Sherlock, S., Kelley, S., Inger, S., Harris, N., Okay, A., " $^{40}\text{Ar}/^{39}\text{Ar}$ and Rb-Sr geochronology of high-pressure metamorphism and exhumation history of the Tavsanlı Zone, NW Turkey. *Contributions to Mineralogy and Petrology*, 137(1), 46-58, 1999.
- [31] Önen, H., "Sub-ophiolite metamorphic rocks from NW Anatolia, Turkey", *Journal of Metamorphic Geology*, 18(5), 483-495, 2000.
- [32] Dilek, Y., Altunkaynak, Ş., "Cenozoic crustal evolution and mantle dynamics of post-collisional magmatism in western Anatolia", *International Geology Review*, 49(5), 431-453, 2007.
- [33] Altunkaynak, Ş., Genç, Ş.C. "Petrogenesis and time-progressive evolution of the Cenozoic continental volcanism in the Biga Peninsula, NW Anatolia (Turkey)", *Lithos*, 102(1), 316-340, 2008.
- [34] Bozkurt, E., "Granitoid rocks of the southern Menderes Massif (southwestern Turkey): field evidence for Tertiary magmatism in an extensional shear zone", *International Journal of Earth Sciences*, 93(1), 52-71, 2004.
- [35] Cunningham-Dunlop I.R., Lee, C., "Technical Report on Kirazlı Gold Property, Çanakkale Province, Turkey, 2007.
- [36] Hunt, G.R., Ashley, R.P., "Spectra of altered rocks in the visible and near infrared" *Economic Geology*, 74(7), 1613-1629, 1979.
- [37] Chang, Z., Yang, Z., "Evaluation of inter-instrument variations among short wavelength infrared (SWIR) devices", *Economic Geology*, 107(7), 1479-1488, 2012.
- [38] Neal, L.C., Wilkinson, J.J., Mason, P.J., Chang, Z., "Spectral characteristics of propylitic alteration minerals as a vectoring tool for porphyry copper deposits. *Journal of Geochemical Exploration*, 184, 179-198, 2018.